Silica particles cause NADPH oxidase–independent ROS generation and transient phagolysosomal leakage

Gaurav N. Joshi, Alexandra M. Goetjen*, and David A. Knecht
Department of Molecular and Cell Biology, University of Connecticut, Storrs, CT 06269

ABSTRACT **Chronic inhalation of silica particles causes lung fibrosis and silicosis. Silica taken up by alveolar macrophages causes phagolysosomal membrane damage and leakage of lysosomal material into the cytoplasm to initiate apoptosis. We investigated the role of reactive oxygen species (ROS) in this membrane damage by studying the spatiotemporal generation of ROS. In macrophages, ROS generated by NADPH oxidase 2 (NOX2) was detected in phagolysosomes containing either silica particles or nontoxic latex particles. ROS was only detected in the cytoplasm of cells treated with silica and appeared in parallel with an increase in phagosomal ROS, as well as several hours later associated with mitochondrial production of ROS late in apoptosis. Pharmacological inhibition of NOX activity did not prevent silica-induced phagolysosomal leakage but delayed it. In Cos7 cells, which do not express NOX2, ROS was detected in silica-containing phagolysosomes that leaked. ROS was not detected in phagolysosomes containing latex particles. Leakage of silica-containing phagolysosomes in both cell types was transient, and after resealing of the membrane, endolysosomal fusion continued. These results demonstrate that silica particles can generate phagosomal ROS independent of NOX activity, and we propose that this silica-generated ROS can cause phagolysosomal leakage to initiate apoptosis.**

Monitoring Editor
Suresh Subramani
University of California, San Diego

Received: Mar 6, 2015
Revised: Jul 13, 2015
Accepted: Jul 14, 2015

INTRODUCTION

Silicosis is caused by the chronic inhalation of large amounts of dust from the environment that contains silica particles (Ross and Murray, 2004). This occurs primarily in various occupational settings and is preventable by wearing a particle mask during exposure. However, in spite of strict Occupational Safety and Health Administration regulations, silicosis continues to occur in workers in the United States and worldwide. In the past few years, exposure to silica dust has particularly increased in individuals involved in hydraulic fracturing (Esswein *et al.*, 2013). Inhalation of silica results in deposition of dust particles in lung alveoli (Oberdörster *et al.*, 2005), where alveolar macrophages scavenge them, resulting in inflammasome activation (Dostert *et al.*, 2008; Hornung *et al.*, 2008) and eventual cell death (Thibodeau *et al.*, 2004; Gilberti *et al.*, 2008; Joshi and Knecht, 2013b). Activated macrophages release the proinflammatory cytokine interleukin-1β (IL-1β), which can initiate the process of fibrosis (Srivastava *et al.*, 2002; Guo *et al.*, 2013) resulting in a reduction in lung function. The death of macrophages that have scavenged silica particles has also been shown to contribute to the process of fibrosis (Borges *et al.*, 2002; Wang *et al.*, 2003).

After particle uptake, the resulting macrophage phagosome undergoes maturation during which it fuses with endosomes and lysosomes that deliver vATPase proton pumps and subunits of the NADPH oxidase 2 (NOX2) complex to the phagosomal membrane (DeLeo *et al.*, 1999; Henry *et al.*, 2004; Suh *et al.*, 2006). The vATPase pumps acidify the phagosomal contents (Lukacs *et al.*, 1990). NOX2 is a multisubunit complex that is activated when the $p47^{phox}$, $p67^{phox}$, and $p40^{phox}$ subunits in the cytoplasm bind to the membrane-associated

This article was published online ahead of print in MBoC in Press (http://www.molbiolcell.org/cgi/doi/10.1091/mbc.E15-03-0126) on July 22, 2015.

*Present address: Genetics and Developmental Biology, University of Connecticut Health Center Graduate School, Farmington, CT 06030,

D.K. designed experiments and cowrote the manuscript; G.J. designed and performed experiments, analyzed data, and cowrote the manuscript; and A.G. performed experiments.

Address correspondence to: David Knecht (David.knecht@uconn.edu).

Abbreviations used: FITC, fluorescein isothiocyanate; H_2HFF, dihydro-2′,4,5,6,7,7′-hexafluorofluorescein; •OH, hydroxyl radical; TRITC, tetramethylrhodamine isothiocyanate.

gp91^{phox} and p22^{phox} subunits (Bedard and Krause, 2007). gp91^{phox} is the catalytic subunit that allows passage of electrons to reduce oxygen to superoxide inside the phagosome. Superoxide is converted to hydrogen peroxide (H_2O_2) by superoxide dismutase or by spontaneous dismutation, and H_2O_2 is neutralized by peroxidases or catalase (Kalyanaraman, 2013). An increase in cytoplasmic and mitochondrial reactive oxygen species (ROS) occurs upon silica exposure (Kang *et al.*, 2000; Fazzi *et al.*, 2014). This increase in ROS can result in NF-κβ activation (Kang *et al.*, 2000) and up-regulation of expression of proinflammatory cytokines that contribute to fibrosis (Rojanasakul *et al.*, 1999).

Crystalline silica has been shown to cause phagolysosomal leakage, and this is hypothesized to be the proximal cause of the induction of the apoptotic cascade (Thibodeau *et al.*, 2004; Joshi and Knecht, 2013a). The release of cysteine and aspartate proteases known as cathepsins has been proposed to activate the inflammasome (Dostert *et al.*, 2008; Hornung *et al.*, 2008) or induce apoptosis (Thibodeau *et al.*, 2004). As noted, phagocytosis leads to ROS production, but the relationship of ROS to vesicular leakage is unclear. Production of ROS is a normal part of the pathway of phagosome maturation, and yet phagosomes containing bacteria or other particles under normal circumstances do not leak and induce apoptosis. One hypothesis for why only silica-containing phagosomes leak relates to Fenton chemistry. Iron contaminating the silica surface might react with phagosomal H_2O_2, forming hydroxyl radical ($^{\bullet}OH$), which can cause lipid peroxidation and might lead to loss of the integrity of the phagosomal phospholipid bilayer (Persson, 2005).

The purpose of this study was to detect the spatiotemporal generation of ROS in cells exposed to silica particles and determine the role of ROS in phagolysosomal leakage and cell death. Various specific and nonspecific ROS probes were used to measure ROS levels inside phagosomes, as well as in the cytoplasm. Latex particles were used as a nontoxic particle control. In macrophages, ROS can be detected in both latex- and silica-containing phagosomes. However, only silica-containing phagosomes transiently leak their contents into the cytoplasm. Of interest, in Cos7 cells, we also detected ROS and leakage in phagolysosome-containing silica in spite of the fact that these cells do not express NOX2. Thus it appears that ROS generated directly by the silica particle surface is sufficient to cause membrane damage and leakage.

RESULTS

Phagocytosis of silica particles results in transient phagolysosomal leakage

Amorphous 3-μm spherical silica particles were used to follow the maturation of individual phagosomes after uptake of particles into cells because their uniform size facilitates visualization of phagosomes. Previous studies showed that both crystalline and amorphous silica particles induce phagolysosomal leakage and apoptosis in alveolar macrophage cell lines (Costantini *et al.*, 2011; Joshi and Knecht, 2013a). To track precisely the timing and extent of leakage, MH-S alveolar macrophages were first allowed to endocytose 4-kDa fluorescein isothiocyanate (FITC)–dextran and 4-kDa tetramethylrhodamine isothiocyanate (TRITC)–dextran to label endosomes and lysosomes (Humphries *et al.*, 2011). The cells were then exposed to 3-μm silica or latex particles and imaged by time-lapse fluorescence microscopy. In this assay, particles are rapidly phagocytosed, and fusion of phagosomes with dextran-containing vesicles is detectable within 5 min of internalization (Gilberti and Knecht, 2015). TRITC fluorescence is pH insensitive and was used to measure the rate and extent of fusion of endosomes with phagosomes, whereas pH-sensitive FITC-dextran fluorescence was used to monitor the pH of the phagosome. The appearance of FITC-dextran fluorescence in the cytoplasm and nucleus is used to measure the extent of phagolysosomal leakage.

Opsonized silica particles are recognized by Fc receptors and rapidly phagocytosed into fluorescent dextran–loaded macrophages. A similar pattern of appearance of dextran fluorescence in phagosomes has been found for every phagosome that has been examined, although the precise timing varies from particle to particle ($n = 20$; a representative example is shown in Figure 1 and Supplemental Movie S1). A frame in which the cell has made contact with a particle before uptake (as determined by the differential interference contrast image) was set as time 0. The cell membrane then extended around the particle and sealed, resulting in the formation of a phagosome. Within a few minutes, both FITC-dextran and TRITC-dextran fluorescence could be detected in the phagosome (Figure 1, A and B, 1–3 min). The porous nature of amorphous silica particles results in the appearance of fluorescent dextran throughout the entire volume of the phagosome. The FITC fluorescence then began to decrease from ~2 min after uptake consistent with acidification of the phagosome (Davis and Swanson, 2010). During this time, the TRITC-dextran fluorescence continued to increase, indicative of continuing delivery of dextran to the phagosome due to fusion of endolysosomes with the phagosome (Figure 1B). Between 24 and 26 min (Figure 1, A and B), an increase in phagosomal FITC-dextran fluorescence was observed. Because the TRITC-dextran fluorescence did not change during this period of time, this is most likely indicative of a rise in phagosomal pH. This result reveals the first step of phagolysosomal leakage, in which phagosomal membrane permeability increases, allowing for the exchange of small molecules with the cytoplasm and thus neutralization of phagosomal pH. Within 1–2 min of the beginning of the increase in FITC-dextran fluorescence, a rapid decrease in both FITC-dextran and TRITC-dextran fluorescence was observed (Figure 1, A and B, 26–30 min). In parallel, an increase in FITC nuclear fluorescence was measured (Figure 1, A at 31 min and B). Surprisingly, within 10 min of the start of leakage, the increase in nuclear FITC-dextran fluorescence ceased, and the phagosomal TRITC-dextran fluorescence began to increase again, indicating that the phagosomal membrane had resealed and endosomes were once again fusing with the phagosome. The increase in phagosomal TRITC-dextran fluorescence continued for nearly 30 min, and during this time, there was no increase in FITC-dextran fluorescence, indicating that the phagosome was also reacidified. The average time over which leakage could be measured was 9 min. A complete quantification of these phagosomal and cellular events is shown in Supplemental Figure S1A. Thus phagolysosomal leakage caused by silica is a transient event, allowing some exchange of material with the cytoplasm, followed by resealing of the phagosomal membrane and then continued fusion with endolysosomes.

To further validate this interpretation of the sequence of events, we prelabeled opsonized silica particles by linking FITC to the opsonizing protein bound to the outside of the particles and exposed them to macrophages preloaded with TRITC-dextran. The fluorescence of particles directly labeled with FITC was also quenched after uptake (3 min onward), consistent with a decrease in phagosomal pH, whereas phagosomal TRITC-dextran fluorescence increased due to fusion of endolysosomes with phagosomes (Supplemental Figure S2A). An increase in FITC fluorescence was seen near the time that TRITC dextran leakage occurred but preceded it by several minutes, indicating an increase in phagosomal pH before TRITC-dextran begins to leak (Supplemental Figure S2, B and

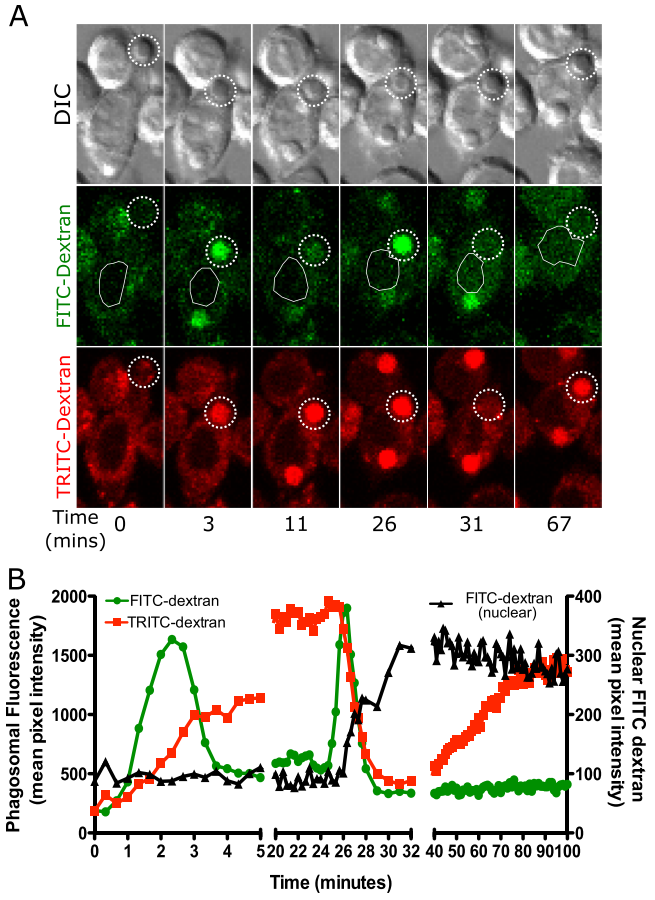

FIGURE 1: Phagosomes containing amorphous silica particles transiently leak some of their contents to the cytoplasm. (A, B) MH-S alveolar macrophages were loaded with 4-kDa FITC dextran and 4-kDa TRITC dextran for 2.5 h and then exposed to 20 μg/cm^2 amorphous, opsonized, 3-μm silica particles. Images were captured through the volume of the cell in 2-μm intervals every 20 s. A plane in which a particle was in focus is shown. (A) In this sequence of images, the particle was phagocytosed and then the phagosome fused with endolysosomes, resulting in an increase in phagosomal fluorescence for both FITC-dextran and TRITC-dextran, as indicated by dotted circle throughout the data set (3 min). FITC-dextran is pH sensitive, and hence, upon acidification, the fluorescence decreased (11 min). On phagolysosome leakage, FITC-dextran fluorescence initially increased due to the influx of cytoplasm (26 min), followed by a decrease in fluorescence due to leakage into the cytoplasm (31 min). This leakage is detected as FITC-dextran signal appearing in the nuclear area of the cell, indicated by a white outline. The TRITC-dextran fluorescence initially continuously increased since it is not affected by the pH change (3–26 min). At the same time that leakage of FITC-dextran occurred, the phagosomal TRITC-dextran fluorescence also rapidly decreased, indicating leakage into the cytoplasm (31 min). This signal was harder to measure in the nuclear area due to signal from the rest of the cytoplasm contributing to nuclear background noise. The TRITC-dextran fluorescence then began to gradually increase beginning at 40 min, presumably due to resealing of the phagosome and continued endosomal fusion. (B) Quantification of data for the cell in A showing data from phagosomal TRITC-dextran and FITC-dextran as well as nuclear FITC-dextran. The trends seen are representative of 20 cells examined.

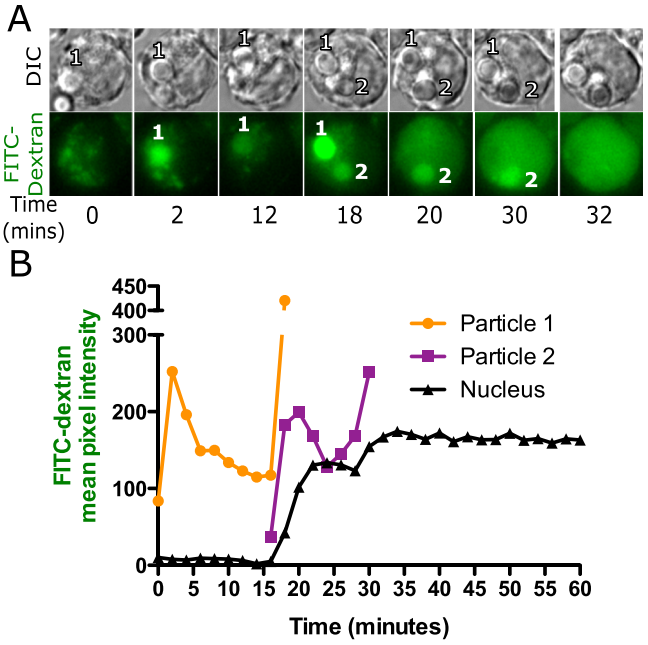

FIGURE 2: FITC-dextran leakage occurs only from a silica-containing phagolysosome. A representative series of images (A) and quantification of the data (B) from a cell loaded with 4- kDa FITC-dextran for 2.5 h and then exposed to a small number of silica particles so that each particle could be tracked. Images were captured 2 min apart on a wide-field epifluorescence microscope. Each particle goes through the same sequence described in Figure 1. Particle 1 showed an initial increase in fluorescence and then a decrease as the FITC-dextran was quenched. At the time of leakage, the phagosome became transiently bright and then dimmer, whereas the nuclear fluorescence increased with a slight delay. Particle 2 showed the same pattern at a later time. Each particle seems to leak only once, but each time a phagosome shows this pattern, there is a correlated increase in nuclear fluorescence. The same quantal changes in nuclear and phagosomal fluorescence were observed in 33 particles in 20 cells.

magnified in C). Phagolysosomal leakage was observed for 6 min based on the decrease in TRITC-dextran phagosomal fluorescence (Supplemental Figure S2B, 18–24 min), after which the TRITC-dextran fluorescence began to increase again, indicating that the phagosome membrane was no longer permeable and endolysosome fusion was continuing.

Because cells often contain multiple silica particles, it was of interest to determine whether the events in one phagolysosome has an effect on other phagosomes/phagolysosomes and cause them to leak simultaneously. Cells were loaded with 4-kDa FITC-dextran and exposed to opsonized silica particles such that most cells received no more than three particles. A sequence of events similar to that in Figure 1A was observed (Figure 2, A and B). Quantification of cells with a small number of phagosomes showed a stepwise increase in nuclear FITC-dextran fluorescence that correlated with specific phagolysosomal leakage events. On phagolysosomal leakage of phagosome 1, an increase in nuclear fluorescence was observed starting at 15 min. A further increase in nuclear fluorescence was not observed until leakage from phagolysosome 2 at 28 min, suggestive of a quantal release of FITC-dextran exclusively from phagolysosomes.

To determine whether nontoxic latex particles also cause phagolysosomal leakage, we exposed MH-S cells loaded with FITC-dextran and TRITC-dextran to 3-μm opsonized latex particles. Because latex particles are not porous, the increase in phagosomal dextran fluorescence is observed only in a ring of fluid between the particle surface and the membrane. A transient increase in

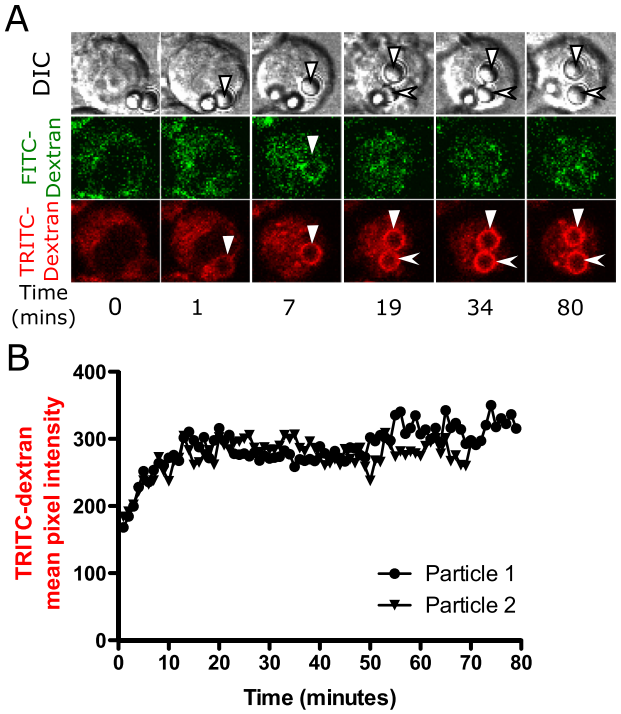

FIGURE 3: Exposure to latex particle does not result in phagolysosomal leakage. Alveolar macrophages were loaded with 4-kDa FITC-dextran and TRITC-dextran (A, B) for 2.5 h, after which they were exposed to 20 μg/cm^2 opsonized 3-μm latex particles. Volumetric image stacks were captured 2 μm apart every minute. (A) A sequence of representative images and (B) quantification of the images. Latex particles are not porous, so the phagosomal fluorescence appears as a ring instead of an entire volume of circle filled with fluorescence. Phagosomes containing latex particles show the same pattern of fluorescence changes as silica phagosomes up to the point of leakage. A brief increase in FITC-dextran fluorescence is observed around the particle at 7 min (marked by solid triangle) before phagosome acidification. (B) Particle 1 (solid triangle) and particle 2 (arrowhead) represent quantified data of particles in the TRITC-dextran channel. These trends are representative of 20 cells examined.

FITC-dextran fluorescence was observed soon after the uptake of latex particles (solid triangle at 7 min in Figure 3A), similar to the results observed with silica particles. A gradual increase in TRITC-dextran fluorescence also occurred; however, phagosomes containing latex particles never showed a later transient increase in FITC-dextran fluorescence, a decrease in TRITC-dextran fluorescence, or an increase in nuclear FITC-dextran fluorescence, indicating that the phagosomal membranes did not become permeable. Instead, the TRITC-dextran fluorescence increased and then plateaued, suggesting that fusion of endolysosomes with the phagosome had ceased.

Particle uptake results in ROS generation in phagosomes

Macrophages have a critical role in innate immunity, as they recognize, phagocytose, and clear foreign material. On phagocytosis, macrophages usually destroy foreign biological material such as pathogens via NADPH oxidase–generated ROS and lysosomal proteases. There are reports of increased ROS generation in cells exposed to silica, and this has been hypothesized to be important in silica-mediated cellular toxicity (Shen *et al.*, 2001; Becher *et al.*, 2007). It is unclear whether the action of ROS is exclusively phagosomal or it also plays a role in the cytoplasm. Some investigators used cytoplasmic probes to examine ROS levels in cells exposed to silica particles (Zeidler *et al.*, 2003). To investigate the source and distribution of ROS in silica-treated cells, several probes were used that were either specific to phagosomes or the cytoplasm.

To examine ROS generation in the phagosome, we conjugated particles with dihydro-2′,4,5,6,7,7′-hexafluorofluorescein (H_2HFF)–bovine serum albumin (BSA) and subsequently opsonized them with anti-BSA antibody. H_2HFF is nonfluorescent but becomes fluorescent upon oxidation. By attaching the dye to particles, we use it as a phagosomal nonspecific ROS sensor. H_2HFF is also pH insensitive, making it an appropriate sensor for detection of phagosomal ROS regardless of the pH (VanderVen *et al.*, 2009). The ability of H_2HFF-labeled silica particles to detect ROS was confirmed by addition of 0.5 M H_2O_2 to medium containing these particles (Supplemental Figure S3). In phagosomes containing H_2HFF-labeled opsonized silica particles, we observed a gradual increase in H_2HFF fluorescence (Figure 4, A and B, particle 1, and Supplemental Movie S2). The fluorescence increased for 25 min after uptake, and then there was a rapid decrease in fluorescence, presumably due to leakage. The H_2HFF is initially linked to BSA, but in the phagosome, the BSA would undergo proteolysis, allowing the H_2HFF to become freely diffusible and leak into the cytoplasm when the phagosomal membrane becomes permeable. We confirmed this by loading MH-S cells with TRITC-dextran and then exposing them to H_2HFF-labeled opsonized silica particles (Figure 4E). On particle uptake, an increase in phagosomal H_2HFF fluorescence was observed along with an increase in TRITC-dextran fluorescence due to endolysosomal fusion. At 24 min, a decrease in H_2HFF fluorescence paralleled the decrease in TRITC-dextran fluorescence, linking both to phagolysosomal leakage. After 25 min, an increase in phagosomal TRITC-dextran fluorescence was measured, indicating that the phagolysosome had resealed and endolysosomal fusion was continuing. However, the phagolysosome no longer had detectable H_2HFF fluorescence. Quantification of other phagocytosed silica particles (particles 2–4) consistently showed ROS detected in the phagosome, followed by phagolysosomal leakage at a later time (Figure 4B). A major concern with time-lapse imaging of oxidation-sensitive dyes is that the fluorescence light source can cause photooxidation of the probe. As a control for this possibility, we also monitored the fluorescence of particles outside of cells. These particles did not show any increase in fluorescence, indicating that periodic exposure to light did not result in photooxidation of H_2HFF (Figure 4, solid triangles in A and C and nonphagocytosed particles in B and D).

To investigate whether ROS generation also occurs in phagosomes containing latex particles, we exposed macrophages to H_2HFF-labeled opsonized latex particles. A gradual increase in H_2HFF fluorescence was also observed in phagosomes containing latex particles (Figure 4C), indicating the presence of phagosomal ROS. This result is expected because activated NOX2 is expected to be associated with all types of phagosomes (Russell *et al.*, 2009; VanderVen *et al.*, 2009). However, unlike silica particles, there was no later loss of fluorescence, indicating no phagolysosomal leakage, consistent with the observation that latex-containing phagosomes did not release TRITC-dextran (Figure 3). Quantification of particle fluorescence shows an increase in H_2HFF fluorescence, reaching a plateau after ~20 min (Figure 4, C and D). Addition of exogenous H_2O_2 to cells led to a further increase in H_2HFF fluorescence, indicating that there was insufficient phagosomal ROS to further oxidize the probe (unpublished data). These data are consistent with other studies showing NOX2 activity tapering off after a short duration (VanderVen *et al.*, 2009). Thus ROS is generated in phagosomes

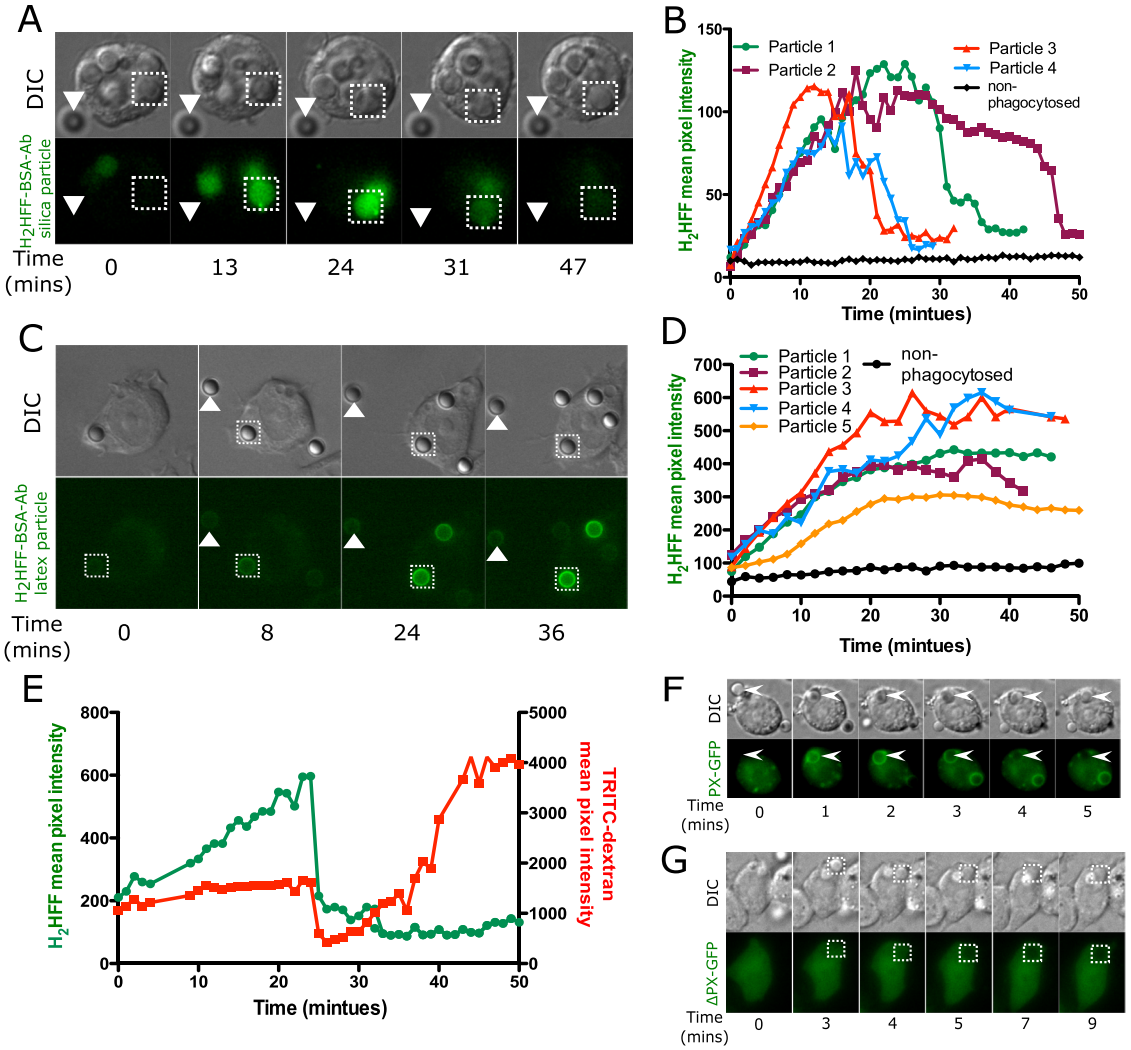

FIGURE 4: Phagosomal ROS is detected upon uptake of silica or latex particles. H2HFF-BSA was coupled to particles, and then the particles were imaged after uptake into MH-S macrophage cells using a wide-field epifluorescence microscope. (A) Phagosomes containing opsonized silica particles labeled with H_2HFF-BSA (square) show an increase in fluorescence indicative of ROS generation. The fluorescence of the phagosome later decreased, indicative of leakage. Nonphagocytosed particles (triangle) did not show any change in fluorescence. (B) Quantification of fluorescence of several particles from several cells. Particle 1 is the particle indicated by the square in A. (C) Latex particles labeled with H_2HFF-BSA also showed an increase in fluorescence (square) indicative of ROS generation. Nonphagocytosed particles (triangle) do not show an increase in fluorescence (control). (D) Quantification of the fluorescence from C and other cells. Particle 1 represents quantification of particle indicated by the square in C. (E) To confirm a decrease in H_2HFF fluorescence observed in A is due to phagolysosomal leakage, macrophages loaded with TRTIC-dextran were exposed to H_2HFF-BSA–labeled silica particles. A decrease in TRITC-dextran and H_2HFF fluorescence was observed simultaneously at 25 min, confirming that the decrease is due to phagolysosomal leakage. (F) MH-S cells were transiently transfected with a vector expressing the PX domain of $p40^{phox}$ fused to GFP (PX-GFP). On uptake of opsonized silica particles, PX-GFP localized around the phagosomes. (G) Cells were transiently transfected with a vector expressing the PX domain, where arginine at position 42 is replaced by glutamine, fused to GFP (ΔPX-GFP), and expressed in macrophages. This probe does not show localization around phagosomes.

containing either silica or latex particles; however, only a phagosome containing a silica particle leaks, implying that either there is a difference in the type of ROS generated or ROS is not the cause of leakage.

Because data are not available regarding assembly of NOX2 on phagosomes in MH-S macrophages, we wanted to confirm that the H_2HFF oxidation observed during particle uptake was consistent with NOX2 activation. The PX domain of $p40^{phox}$ fused to green fluorescent protein (PX-GFP) was expressed in MH-S cells, and localization of the probe after particle uptake was visualized. The PX domain of $p40^{phox}$ binds to phosphatidylinositol 3-phosphate (PI(3)P) on phagosomal membranes, allowing the tethering of the cytoplasmic trimeric oxidase complex to the membrane. The appearance of PX-GFP on phagosomes is indicative of assembly of the NOX2 complex (Ellson *et al.*, 2006; Tian *et al.*, 2008). On phagocytosis of opsonized silica particles, PX-GFP was recruited onto phagosomes within 1 min but was undetectable after 4 min (Figure 4F). To confirm this interpretation, we expressed ΔPX-GFP containing a R58A mutation that prevents binding of the PX domain of $p40^{phox}$ to PI(3)P in macrophages. Localization of ΔPX-GFP to

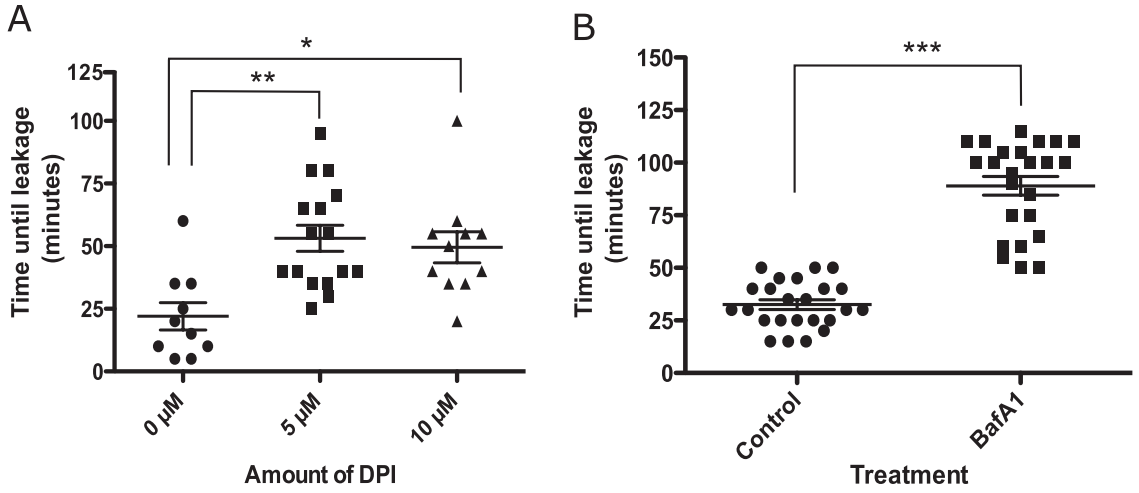

FIGURE 5: Effect of pharmacological inhibitors on phagolysosomal leakage. (A) Cells were loaded with 4-kDa FITC-dextran for 2.5 h, and, after a wash of dextran, cells were incubated with inhibitors for 30 min, after which they were exposed to opsonized silica particles. The time it took for an individual phagolysosome to leak FITC-dextran after particle uptake was measured. (A) After treatment with the NADPH oxidase inhibitor DPI (0, 5, and 10 μM), average time for phagolysosomal leakage increased from 25 to 60 min. $^{**}p < 0.001$ and $^{*}p < 0.01$ (B) After treatment with 150 nM bafilomycin A1 (a vATPase inhibitor), average time for phagolysosomal leakage increased from 30 to 90 min. $^{***}p < 0.0001$. Bar represents mean ± SEM of multiple phagolysosomal leakage events for each treatment type.

phagosomes was not observed after particle uptake into cells (Figure 4G).

Alterations in the phagosomal milieu delay phagolysosomal leakage

If NOX2-generated ROS contributes to membrane damage and leakage in silica-containing phagosomes, then inhibiting NOX2 activity or changing the phagosomal environment may alter the leakage process. To alter ROS production, we preloaded macrophages with 4-kDa FITC-dextran and then treated them with diphenyleneiodonium (DPI) before exposure to silica particles. DPI binds to FAD, inhibiting its ability to transfer electrons via $gp91^{phox}$ into the phagosomal lumen, thus inhibiting superoxide formation (Savina *et al.*, 2006). The time it took for an individual phagolysosome to leak after particle uptake was measured in cells treated with different concentrations of DPI. In untreated cells, the average time for phagolysosomal leakage was 25 min, which increased to 55 min upon pretreatment with 5 μM DPI (Figure 5A). Increasing the concentration of DPI to 10 μM did not prolong the time of phagolysosomal leakage further. Thus NOX2 inhibition did not prevent leakage but instead delayed it.

One hypothesis to explain the link between ROS and leakage is that phagosomal ROS is being converted from superoxide to some more damaging species in the presence of silica. Because conversion of superoxide to hydrogen peroxide is facilitated by H^+ ions (Fisher, 2009; Winterbourn and Kettle, 2013), we reasoned that blocking proton flux might inhibit the generation of the damaging ROS and thus prevent phagolysosomal leakage. The acidic pH of the phagosome is maintained by protons that are transported into the lumen by vATPase (Lukacs *et al.*, 1990). Cells preloaded with 4-kDa FITC-dextran were pretreated with bafilomycin A1, an inhibitor of vATPase, to prevent phagosomal acidification. As expected, after treatment with bafilomycin A1, there was an unquenching of FITC-dextran fluorescence, confirming an increase in pH in vesicles containing FITC-dextran (unpublished data). Surprisingly, inhibition of phagosomal acidification was more potent in preventing phagolysosomal leakage than inhibition of NOX2 activity. On exposure to silica particles, the average time it took for an individual phagosome to leak after particle uptake increased from 25 to 100 min (Figure 5B).

Silica can induce phagolysosomal leakage in the absence of NADPH oxidase

Data from NOX2 inhibition experiments suggested that phagolysosomal leakage might occur independently of NOX2 activity. We tested this hypothesis by studying phagolysosomal leakage in Cos7 cells, which do not express NOX2 or show any detectable NOX activity (Price *et al.*, 2002). Cos7 cells also lack the FcγRIIA receptor involved in recognition of opsonized particles. Instead, nonopsonized (BSA-coated) silica particles were used, since these particles have been shown to be internalized by Cos7 cells (Costantini *et al.*, 2011). Cos7 cells were allowed to endocytose TRITC-dextran and then exposed to nonopsonized silica particles. On particle uptake, a gradual increase in phagosolysosomal TRITC-dextran fluorescence was observed similar to what was seen in MH-S macrophages (Figure 6A up to 85 min). The phagolysosomal fluorescence then transiently decreased, indicative of phagolysosomal leakage (85–90 min), and then began to increase again, indicative of membrane sealing and continued endosome fusion (95 min onward, Figure 6A). Quantification of the particle fluorescence in Figure 6A is shown in Figure 6B. Quantification of fluorescence changes for other particles reveals that leakage happens consistently, but there is heterogeneity in the timing of leakage similar to that seen in MH-S cells (Figure 6C). Thus phagolysosomal leakage can also occur independent of NADPH oxidase. Phagolysosomal leakage in Cos7 cells was also confirmed using the FITC-dextran leakage assay. An increase in phagosomal FITC-dextran fluorescence was detected, indicating an increase in phagosomal pH. Subsequent leakage of individual phagolysosomes resulted in a quantal increase in FITC-dextran fluorescence in the cytoplasmic and nuclear area (Supplemental Figure S4).

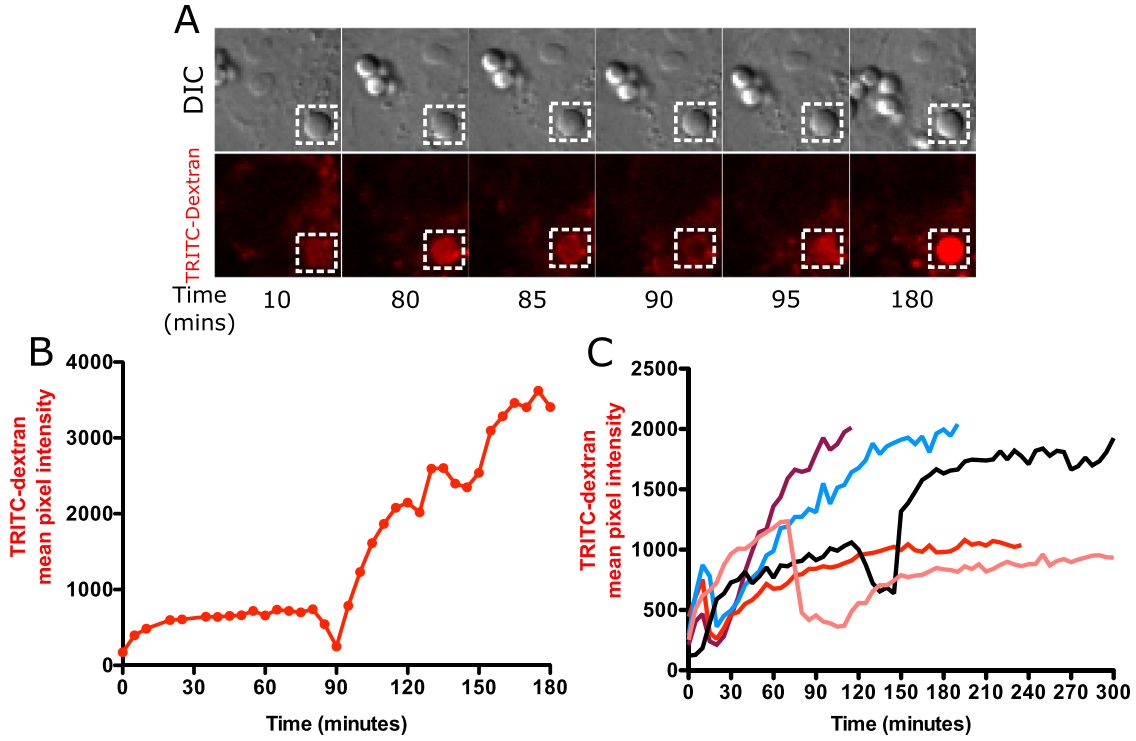

FIGURE 6: Phagolysosomal leakage occurs in Cos7 cells exposed to silica particles. (A) Cos7 cells loaded with 4-kDa TRITC-dextran were exposed to 20 μg/cm^2 nonopsonized silica particles and imaged at 5-min intervals. Note that Cos7 cells take a long time to initiate the process of phagocytosis after exposure to particles. Images were therefore acquired at 5-min intervals to prevent any inhibition of particle uptake due to excessive photoexposure. The phagolysosomal leakage data for Cos7 cells therefore lack a comparable temporal resolution to that of MH-S cells, where particle uptake is rapid and images were acquired 20 s apart. A gradual increase in TRITC-dextran fluorescence was observed upon particle phagocytosis (10 and 80 min), followed by a decrease in fluorescence starting at 85 min, with maximum loss of signal observed at 90 min. Vesicle refusion starts at 95 min, leading to a subsequent gradual increase in TRITC fluorescence. (B) Quantification of the phagosome in A. (C) Phagolysosomal leakage of individual phagosomes from different cells.

ROS is detected in Cos7-cell phagosomes containing silica but not latex particles

It was surprising that leakage occurred in Cos7 cells after phagocytosis of silica particles. It has been presumed that ROS from NOX2 plays a central role in membrane damage leading to leakage. The fact that leakage occurs in the absence of NOX2 activity led us to test the possibility that the silica surface was generating ROS directly. To address this possibility, we loaded Cos7 cells with 4-kDa TRITC-dextran and then exposed them to H_2HFF-BSA–coated silica or latex particles. On silica particle uptake, a general trend was observed in which there was an increase in both TRITC-dextran and H_2HFF phagosomal fluorescence, suggestive of phagosome–endolysosome fusion and ROS generation, respectively. For the particle marked by the arrowhead in Figure 7A, there was an increase in H_2HFF fluorescence from 0 to 100 min, whereas TRITC-dextran fluorescence increased briefly after uptake and then plateaued. At 440 min, there was a small increase in H_2HFF fluorescence, indicative of ROS generation, followed by a simultaneous decrease in TRITC-dextran and H_2HFF fluorescence, indicative of leakage (Figure 7, A and B). Postleakage endolysosomal fusion was then observed during which a large increase in TRITC-dextran fluorescence occurred from 455 to 550 min (Figure 7, A and B). A representative trend for a second particle shows an increase in H_2HFF fluorescence followed by leakage of TRITC-dextran (solid triangle, Figure 7, A and C). Particles that were not phagocytosed do not show an increase in H_2HFF fluorescence, indicating that light exposure did not result in photooxidation of the dye (Supplemental Figure S5A). These data were quantified, as imaging was performed for several hours on Cos7 cells compared with MH-S macrophages, where this was done for 1 h.

To validate whether the observed ROS generation was specific to silica particles, we exposed Cos7 cells loaded with 4-kDa TRITC-dextran to H_2HFF-BSA–labeled latex particles. The increase in TRITC-dextran fluorescence around a latex particle (Figure 7, D and E) in Cos7 cells occurred in a manner similar to that of silica particles and latex particles in MH-S cells (Figure 3, A and B). Further, there was no decrease in TRITC-dextran fluorescence, indicating that latex particles do not result in phagolysosomal leakage in Cos7 cells. Whereas TRITC-dextran fluorescence continued to increase during phagosome maturation, an increase in H_2HFF fluorescence was not observed, indicating that ROS was not detectable in Cos7 phagosomes containing latex particles (Figure 7, D and E). Because nonopsonized latex particles were used for Cos7 cells and opsonized latex particles for MH-S cells, it is possible that a lack of ROS generation could stem from a difference in particle coating. MH-S cells were therefore exposed to nonopsonized latex particles labeled with H_2HFF. They showed an increase in H_2HFF fluorescence, indicating that ROS generation in a macrophage phagosome is not related to the antibody or protein coating on a particle (Supplemental Figure S6, A and B). Thus Cos7 cells are unable to generate ROS upon phagocytosis of latex particles due to the absence of

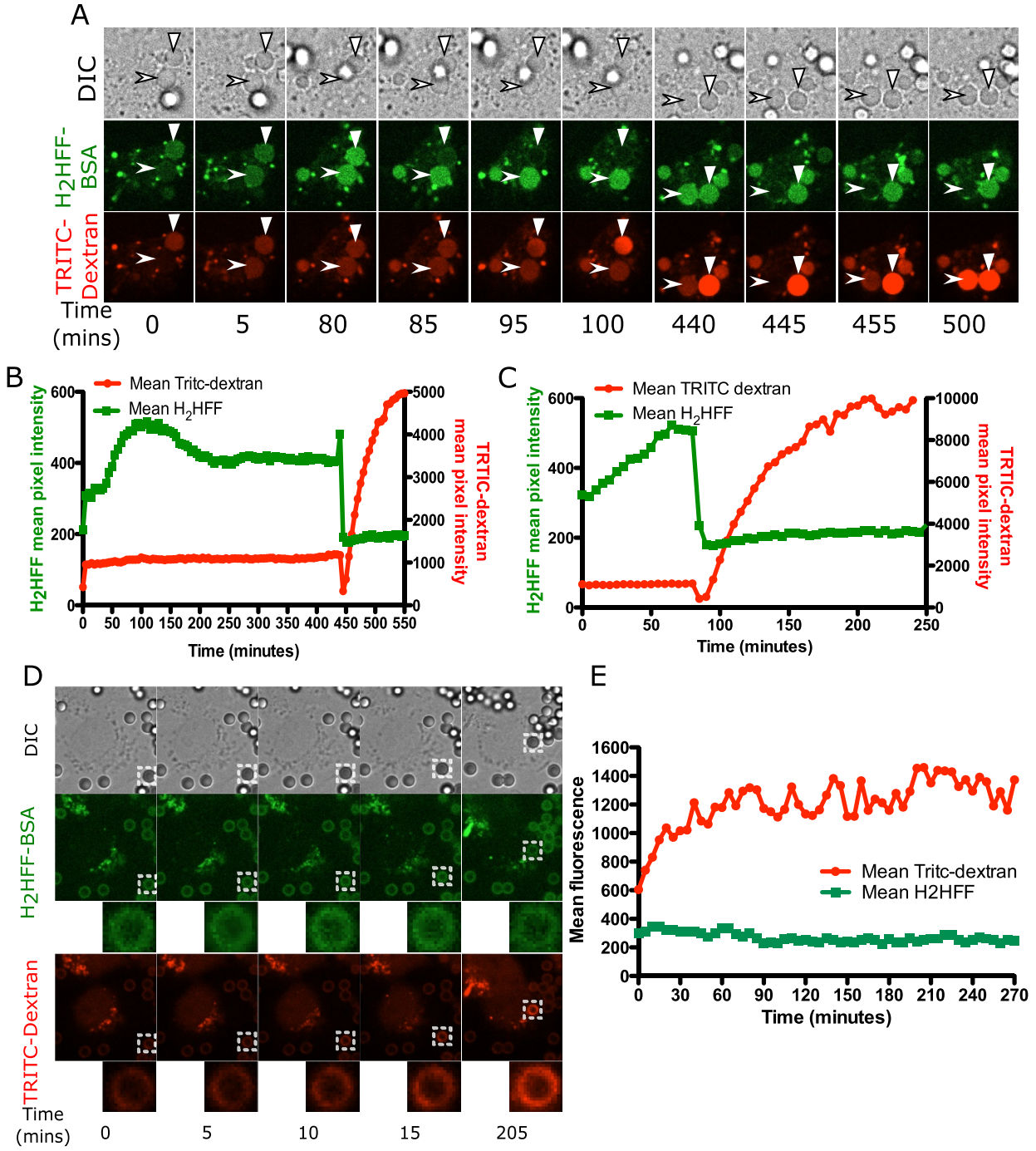

FIGURE 7: ROS in Cos7 cells is detected in phagosomes containing silica particles but not latex particles. (A) Cos7 cells loaded with 4-kDa TRITC-dextran were exposed to 20 μg/cm^2 H_2HFF–labeled, nonopsonized silica particles and imaged at 5-min intervals. On uptake, an increase in TRITC-dextran fluorescence as well as H_2HFF fluorescence was observed for both phagosomes, marked by arrowhead and solid triangle. For a phagolysosome marked by an arrowhead, at 445 min, a decrease in H_2HFF and TRITC-dextran fluorescence due to phagolysosomal leakage was observed. After leakage, a gradual increase in TRITC-dextran fluorescence was observed, consistent with continued endosome fusion. However, H_2HFF fluorescence remained low, as expected, since the dye has leaked out of the phagosome. The particle labeled by a solid triangle was already phagocytosed when imaging began, and hence it is already labeled by TRITC-dextran at 5 min, whereas a gradual increase in H_2HFF fluorescence is observed. At 85 min, a decrease in both H_2HFF and TRITC-dextran fluorescence was observed, indicative of phagolysosomal leakage. From 95 min onward, a gradual increase in TRITC-dextran fluorescence was observed, indicative of endosome fusion. (B) Quantification of fluorescence of the particle indicated by an arrowhead. (C) Quantification of fluorescence of the particle indicated by the solid triangle. (D) Cos7 cells loaded with 4-kDa TRITC-dextran were exposed to 20 μg/cm^2 H_2HFF-labeled, nonopsonized latex particles and imaged at 5-min intervals. Whereas an increase in TRITC-dextran fluorescence around the latex phagosomes was observed over time, no increase in H_2HFF fluorescence was measured. (E) Quantification of the fluorescence of the particle in D. Representative of 20 individual phagosomes.

NOX2, whereas silica particles are able to generate NOX-independent ROS.

An increase in cytoplasmic ROS occurs only in silica-treated cells

Silica-induced ROS generation results in up-regulation of NF-κB and production of proinflammatory cytokines (Rojanasakul *et al.*, 1999; Kang *et al.*, 2000). These cytokines play a role in progression of disease pathology and development of fibrosis. It has been proposed that this ROS is a result of NOX activation and is responsible for cell death (Sato *et al.*, 2008). Relating NOX2 activation to cytoplasmic ROS and to cell death upon silica exposure has been difficult due to lack of reliable ROS probes and appropriate hardware allowing long time-lapse measurements without affecting cells. We measured the generation of nonspecific and specific ROS in the cytoplasm upon exposure of macrophages to silica and latex particles to determine whether cytoplasmic ROS is due to NOX2 activity and whether the particle type affects the presence of cytoplasmic ROS.

Alveolar macrophages were loaded with CM-H_2DCFDA, which localizes to the cytoplasm and oxidizes to the fluorescent product DCF in the presence of many types of ROS. MH-S cells exposed to latex particles did not show any increase in CM-H_2DFCDA fluorescence, whereas cells exposed to silica particles showed an increase in cytoplasmic fluorescence within 30 min (Figure 8B). Thus cytoplasmic ROS generation is not due solely to NOX activity but is also dependent on particle type. Time-lapse imaging of cells exposed to silica particles also shows a later increase in ROS during the final stages of apoptosis when cell shrinkage (cell 1, 170 min, Figure 8A) or cell blebbing occurs (cell 1, 250 min onward, Figure 8A). Similar results were observed for other cells (e.g., cell 2, 600 min and onward, Figure 8, A and C). Thus a two-step increase in cytoplasmic CM-H_2DCFDA fluorescence is observed: a small increase after exposure to silica but not latex particles, and another increase during late stages of apoptosis.

CM-H_2DCFDA is a nonspecific ROS sensor, and one of the ROS it detects is H_2O_2 (Morgan *et al.*, 2011; Kalyanaraman *et al.*, 2012). To specifically detect H_2O_2 and confirm these results with a different probe, we transfected MH-S cells with the genetically encoded ratiometric ROS sensor roGFP2-Orp1 (Morgan *et al.*, 2011). Fusion of a redox-active GFP (roGFP2) with Orp1, a thiol peroxidase, makes this probe highly selective for H_2O_2. Cells exposed to silica particles showed an increase in ROS within the first 2 h after particle uptake, whereas there was no change in cells taking up latex particles (Figure 8E). On tracking a cell until death, a huge increase in ROS was observed upon cell blebbing (cell 1, 270 min and onward, Figure 8D). Quantification for cell 1 and cells 2–5 reveals a similar outcome to that with the CM-H_2DCFDA probe. A small increase in ROS is seen soon after silica particle uptake and a much larger increase during secondary necrosis (Figure 8F). Thus the results with roGFP2-Orp1 are similar to those found with the CM-H_2DCFDA probe.

An elevation in ROS during later stages of apoptosis has been proposed to be due to mitochondrial dysfunction. To confirm that the late increase in ROS observed with CM-H_2DCFDA and roGFP2-Orp1 correlates with an increase in mitochondrial ROS, we transfected cells with mito-roGFP2-Orp1 to detect H_2O_2 generated in mitochondria. This probe detected an increase in mitochondrial ROS only after a cell started to bleb (390 min and onward, Figure 8G). Quantification of several cells shows a similar trend in which an increase in ratio is observed only upon initiation of cell blebbing (Figure 8H). Thus it is likely that the cytoplasmic ROS detected during apoptosis is generated in mitochondria and not related to silica particles directly.

The pathway of events upon cellular uptake of silica particles

Examination of many cells and particles led to a proposed model of the molecular events that unfold after silica particle phagocytosis (Figure 9). The endolysosomes preloaded with 4-kDa FITC-dextran and 4-kDa TRITC-dextran are represented by yellow vesicles (stage 1). Opsonized or nonopsonized silica particles bind to the cell and are taken up into phagosomes (stages 2 and 3). Endolysosomal vesicles then begin to fuse with the phagosome (stage 3), delivering their contents to the phagosome, now referred to as a phagolysosome (stage 4). vATPases present on the endolysosomal vesicles pump protons into the phagolysosomal lumen, resulting in a pH decrease and hence a decrease in the fluorescence of pH-sensitive FITC-dextran, so that phagosomes are now red. At the same time, the NOX2 activity results in ROS generation within the phagolysosome lumen (stage 5). ROS can also be detected in the cytoplasm before phagolysosomal leakage. After ~25 min, there is phagolysosomal membrane permeability, leading to an increase in the pH of the phagolysosome (stage 6). Within 1.5 min, the leakage of both FITC-dextran and TRITC-dextran into the cytoplasm can be detected (stage 7). After ~10 min, the leaky phagolysosome is resealed, during which the dextran begin to accumulate in the phagolysosome due to endolysosomal fusion. Only the TRITC-dextran fluorescence is detected because the phagolysosome is again at a low pH due to vATPase activity (stage 8). During phagolysosomal leakage, the cathepsins or other molecules released from the lumen lead to activation of the inflammasome, Il-1β release (Dostert *et al.*, 2008; Hornung *et al.*, 2008), and, after several hours, initiation of apoptosis (Joshi and Knecht, 2013b). In latex-containing phagosomes, the same early events take place, except that no leakage occurs and no cytoplasmic ROS can be detected. In Cos7 cells, the same events (stages 1–8) take place but without NOX2-generated ROS.

DISCUSSION

Phagocytosis of foreign material and generation of phagosomal ROS to kill pathogens are essential functions of the innate immune system. There is no evidence that phagosomal ROS generated in this process results in phagolysosomal membrane damage and or that there is any leakage of phagosomal contents into the cytoplasm. However, it is clear that phagocytosis of silica particles results in phagolysosomal leakage. ROS generation was previously measured in cells exposed to silica particles, but these studies did not provide information regarding the source or intracellular distribution of ROS. We therefore investigated whether ROS generated by NOX2 in a phagosome was responsible for phagolysosomal leakage. In this study, we show that the NOX2-dependent oxidative burst associated with phagocytosis in macrophages accelerates the process of silica-induced phagolysosomal leakage, but leakage can also occur independently of NOX2. In macrophage cells, both toxic silica and nontoxic latex particles cause the activation of NOX2 on phagosomal membranes, resulting in the production of phagosomal ROS. Only silica particles cause an increase in cytoplasmic ROS, and this occurs at roughly the same time as ROS is detected in the phagosome but before leakage is detected. This implies that this particular ROS, unlike NOX2-generated ROS, is able to escape from the phagosome. Unfortunately, there are not sufficient specific ROS probes to determine precisely the molecular nature of this ROS. We show that NOX2 is neither necessary nor sufficient for phagolysosomal leakage but appears to play a role in toxicity by accelerating the timing of leakage.

Opsonized particle phagocytosis is a complex process orchestrated by various effector molecules upon engagement of Fc receptors on the surface of cells by antibody-coated particles (Aderem and Underhill, 1999). An alternate way of particle uptake is by nonspecific recognition of proteins on the surface of the particles. The binding and clustering of Fc receptors in the case of opsonized particles or nonspecific binding to protein-coated nonopsonized particles leads to localized actin polymerization and the engulfment and internalization of particles to form a phagosomal vesicle (Swanson and Hoppe, 2004; Scott, 2005; Bohdanowicz *et al.*, 2010; Gilberti and Knecht, 2015). The phagosome undergoes maturation by fusing with endosomes and lysosomes to deliver, among other things, the vATPase that causes the luminal pH to be lowered and lysosomal enzymes to become activated (Bohdanowicz and Grinstein, 2010).

Our study using dual dextran fluorescent tracers reveals for the first time the kinetics of phagolysosomal leakage. The increase in pH of the phagosome occurs several minutes before we can detect any leakage of dextran into the cytoplasm. There are two possible explanations for this result. The size of the pore might initially be large enough to allow protons to cross the membrane but not large enough to allow dextran through. Over time, the pore might enlarge and begin allowing dextran and other larger molecules to pass. Alternatively, the difference in diffusion rate of protons versus larger molecules through a fixed-size pore might be sufficient to account for the different kinetics. We favor an increase in the size of pores over time, as there is a span of several minutes during which the FITC-dextran fluorescence is increasing while there is no detectable decrease in the TRITC-dextran fluorescence (Figure 1). The parallel timing seen between the decrease in TRITC-dextran and FITC-dextran fluorescence in the phagolysosome and a simultaneous increase in its nuclear fluorescence supports the idea that we are accurately measuring leakage with this assay. Note that our earlier studies showed that dextran as large as 70 kDa can leak out of phagolysosomes (Joshi and Knecht, 2013b). A pore of this size is consistent with the size of proteins such as cathepsins that are suspected to induce the apoptotic cascade once released into the cytoplasm. Note that the mode by which molecules cross the phagolysosomal membrane is unknown. Whether it is purely a lipid bilayer phenomenon or involves membrane proteins is unknown, as well as whether lipid peroxidation by ROS plays a role in its formation. There is very little biophysical data or modeling to explain the molecular details of the formation of transient membrane pores (Wong-Ekkabut *et al.*, 2007). Although we have referred to it as a "pore," we do not have any evidence on the number, size, or nature of the permeable region of the membrane.

Surprisingly, we found that phagolysosomal leakage is a transient event. The leakage of 4- kDa dextran takes place for an average of 9 min and then stops. After this time, TRITC-dextran fluorescence begins to increase in the phagosome, indicating that leakage has stopped and the fusion of endolysosomes with the phagosome has continued throughout the period of leakage or has begun again. We never saw a phagosome in a macrophage leak once and then subsequently leak again or ever saw one leak its contents and not recover. This resealing of leaky phagolysosomal membranes was observed with both opsonized and nonopsonized silica particles. After a period of increase, TRITC-dextran fluorescence was seen to level off for latex phagosomes and sometimes for silica-containing phagosomes before leakage (Figures 3 and 6). Thus fusion with endolysosomes often ceases after some period of time. However, upon leakage of phagosomes containing silica, a further increase in TRITC-dextran fluorescence was always observed, implying renewed fusion events. Thus we hypothesize that release of phagolysosomal contents may trigger recruitment of endolysosomal vesicles, and this new membrane may help repair the damaged phagolysosomal membrane. Recently autophagic machinery was found to be localized to damaged lysosomes, suggesting sequestration of damaged phagolysosomes by autophagosomes (Maejima *et al.*, 2013), so this may be a related process. We cannot ascertain whether TRITC-dextran that was endocytosed by cells during loading also got mixed with autophagosomes that are generated de novo. A leaky phagolysosome could therefore be sealed by an autophagosome or possibly by other endolysosomal vesicles.

Although ROS was detected in phagosomes containing either silica or latex particles, only silica-containing phagosomes become damaged and leaked, leading eventually to cell death (Thibodeau *et al.*, 2004; Joshi and Knecht, 2013b). One hypothesis to explain more-toxic ROS in the presence of silica relates to iron contamination of the silica surface. Crystalline silica particles that cause silicosis have been shown to have traces of iron (Vallyathan *et al.*, 1988; Ghio *et al.*, 1992; Castranova *et al.*, 1997). A micro–x-ray fluorescence analysis of amorphous silica particles used in this study confirmed traces of iron on them (unpublished data). Phagosomal H_2O_2 generated by reduction of superoxide could be converted to $^{\bullet}OH$ via ferrous (Fe^{2+}) iron in a process known as the Fenton reaction (Kurz *et al.*, 2011). This reaction has been demonstrated using electron paramagnetic resonance spectroscopy, in which a free radical trap (DMPO) forms a stable adduct with the $^{\bullet}OH$ (DMPO-OH), allowing the detection of short-lived and highly reactive $^{\bullet}OH$ (Hampton *et al.*, 1998). A suitable fluorescence probe to detect $^{\bullet}OH$ is not available, making it difficult to detect this ROS in a phagosome using fluorescence microscopy. Within the phospholipid bilayer of a phagosome, $^{\bullet}OH$ can react with polyunsaturated fatty acids, resulting in the formation of lipid hydroperoxide, causing a reduction in membrane fluidity, and increasing the permeability of the lipid bilayer (Wong-Ekkabut *et al.*, 2007). However, whether this would lead to transient pores large enough to allow dextran or proteins to diffuse through and how those pores are subsequently closed are unknown.

An argument against toxicity due to iron is that iron is present in lysosomes (Kon *et al.*, 2010), and so it is hard to imagine why the Fenton chemistry would not also take place in phagolysosomes containing latex particles. Much of this iron is in a redox-active form but sequestered by the protein ferritin. However, some of the free iron in lysosomes can participate in redox reactions (Kurz *et al.*, 2011). Owing to the high reducing equivalence of proteins and the acidic nature of lysosomes, most of the free iron has been proposed to be present in the Fe^{2+} form. However, ferrous (Fe^{2+}) and ferric (Fe^{3+}) iron can interconvert, and superoxide can reduce ferric iron to ferrous (Kon *et al.*, 2010; Kurz *et al.*, 2011; Dixon and Stockwell, 2013). Thus, if Fenton chemistry were important, one would hypothesize that phagocytosis of latex particles would also result in generation of $^{\bullet}OH$ and cause phagolysosomal membrane leakage. Our data strongly suggest that even if these reactions occurred in a latex phagolysosome, the resulting ROS would not be not sufficient to cause damage to phospholipid bilayer. It is only in the presence of silica that something abnormal happens. We hypothesize this event to be the silica-dependent de novo generation of a form of ROS that is particularly damaging to nearby membrane bilayers.

One way of knowing whether phagolysosomal leakage was due to ROS generation was by blocking it at its source (NADPH oxidase) or before H_2O_2 generation, a step that requires protons pumped into the phagosome by vATPase (Winterbourn *et al.*, 2006; Musset *et al.*, 2009). DPI and bafilomycin A1, inhibitors of NOX and vATPase,

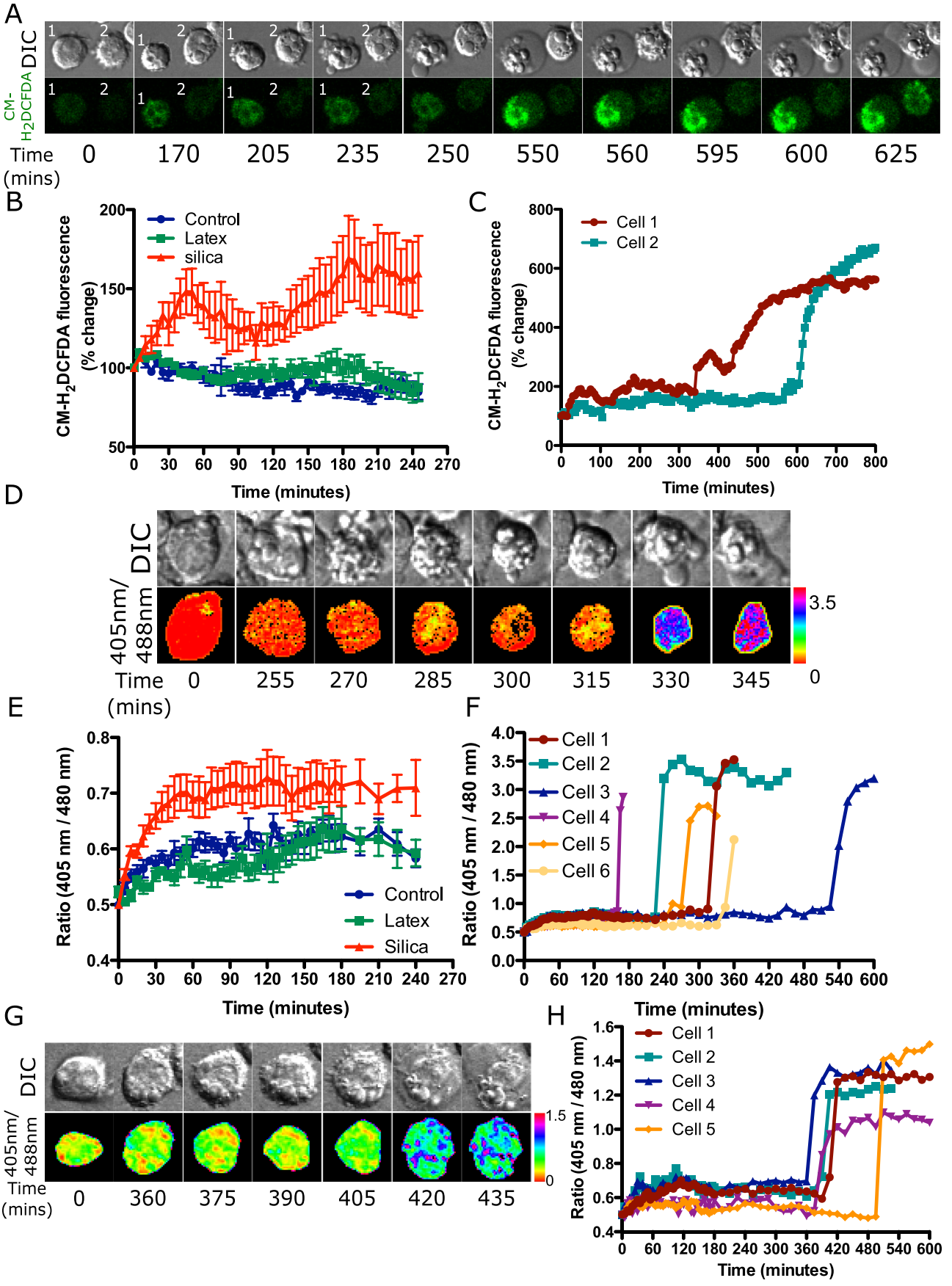

FIGURE 8: Cytoplasmic ROS is detected in MH-S cells exposed to silica but not latex particles. MH-S cells were plated in an eight-well chambered slide and labeled with 10 μM CM-H_2DCFDA, and four fields per well were imaged 5 min apart after exposure to either opsonized silica particles or latex particles (A–C). (A) A small increase in fluorescence is

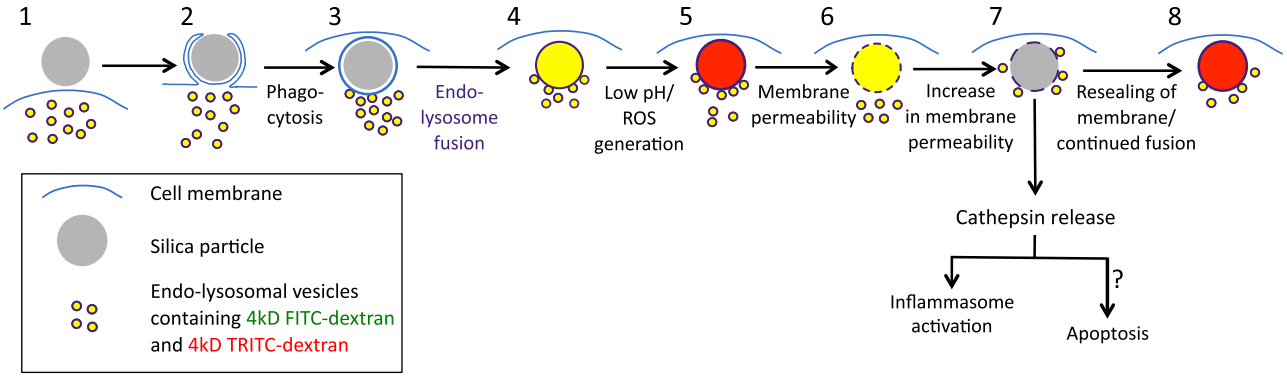

FIGURE 9: Pathway of cellular events upon uptake of silica particles.

respectively, present an opportunity to investigate the role of ROS in leakage (Savina *et al.*, 2006; Hornung *et al.*, 2008; Sandberg *et al.*, 2012). In one study, DPI-treated macrophages exposed to silica prevented phagolysosomal leakage (Persson, 2005). This was significant because it suggested a necessary role of NOX2- generated ROS in silica-induced phagolysosomal leakage. In another study in which DPI-treated macrophages were exposed to silica particles, partial release of FITC-dextran was observed after fixed time period of 1 h (Davis *et al.*, 2012). Our data for DPI-pretreated macrophages exposed to silica particles show a temporal delay in release of FITC-dextran from individual phagolysosome. This supports the observation of Davis *et al.* (2012) and further shows that the reason for partial release is a delay in phagolysosomal leakage. Treatment of bone marrow–derived macrophages with bafilomycin A1 resulted in reduced generation of IL-1β upon silica treatment (Hornung *et al.*, 2008). Our data on bafilomycin A1–treated macrophages exposed to silica show a delay in phagolysosomal leakage. Reduced generation of IL-1β could therefore be due to a delay in phagolysosomal leakage that is required for inflammasome activation and subsequent IL-1β release. Neither of these inhibitors could be tested for their ability to prevent cell death after leakage, as they cause cell death on a shorter time scale than silica. Both DPI and bafilomycin A1 were used to investigate any reduction in phagosomal ROS upon exposure to silica particles. Even in the presence of DPI, H_2HFF oxidation occurred in phagosomes containing silica. This is not surprising, as silica can generate ROS in the absence of NOX2 in a Cos7 cell phagosome. However, we have no way to calibrate the phagosomal H_2HFF signal to know how much of a decrease in ROS would be needed to see a change in H_2HFF fluorescence. Bafilomycin A1, surprisingly, caused an increase in cellular fluorescence that made it difficult to detect the H_2HFF signal, making it impossible to determine whether there was a decrease in phagosomal ROS.

Because Cos7 cells also lack Fc receptors, they cannot use the opsonized phagocytosis pathway of phagocytes for uptake of antibody-coated particles. However, we have shown that macrophages and nonphagocyte cell types can take up nonopsonized particles (Costantini *et al.*, 2011; Gilberti and Knecht, 2015). In Cos7 cells, uptake of nonopsonized particles is much slower than in macrophages, but particles are eventually taken up, and silica particles cause phagolysosomal leakage. These data are consistent with the observation from a previous study that showed silica particles could induce phagolysosomal leakage independent of NOX2 (Davis *et al.*, 2012). Our data also support the observation that silica can generate ROS in a phagosome in a NOX2-independent manner. Cos7 cells do not express NOX2, but other isoforms of NOX could conceivably contribute to phagosomal ROS. However, the fact that ROS was detected in silica-containing phagosomes but not latex-containing phagosomes in Cos7 cells indicates that other NOX isoforms do not contribute to measurable phagosomal ROS. Phagolysosomal leakage independent of NOX2 could explain why silica-treated bone marrow–derived macrophages from gp91^{phox}-knockout mice resulted in inflammasome activation and release of IL-1β (Hornung *et al.*, 2008).

observed over time in cells 1 and 2 upon particle addition, which remains constant up to 250 min for cell 1 and 600 min for cell 2 (quantified in C). A further increase in fluorescence is observed after cell blebbing during secondary necrosis (cell swelling) at 550 min for cell 1 and 625 min for cell 2. (B) Comparison of the change in CM-H_2DCFDA fluorescence in control cells and upon exposure to latex or silica particles showing that only silica results in the generation of measurable cytoplasmic ROS. Data represent the mean ± SEM of at least 10 individual cells for each treatment type. (C) Quantification for cells 1 and 2 in A showing a small increase in fluorescence after particle addition as opposed to the huge increase in ROS generation during cell death. (D–F) To detect specifically H_2O_2 in cells, MH-S cells expressing roGFP2-Orp1 were exposed to either opsonized silica or latex particles and imaged at 5-min intervals. (D) A small increase in roGFP2 ratio is observed in first hour; however, this cannot be represented in the ratiometric images. After cell blebbing, a huge change in roGFP2 ratio is observed at 330 min. (E) Comparison of the change in roGFP2-Orp1 ratio in control cells and upon exposure to latex or silica particles showing that only silica results in the generation of measurable cytoplasmic H_2O_2. Data represent mean ± SEM of at least 10 individual cells for each treatment type. (F) Quantification for the cell in D is represented by cell 1, and other cells are represented as 2–6. All of these cells show a huge increase in ratio at different time points, which relates to cell death. (G) To detect mitochondrial H_2O_2, MH-S cells expressing mito-roGFP2-Orp1 were exposed to opsonized silica particles. In pseudocolored ratiometric images, mitochondria appear red to yellow, indicative of basal H_2O_2, whereas upon secondary necrosis, there is an increase in H_2O_2 from 420 min onward; mitochondria appear blue to pink. (H) Quantification of cell represented in G, cell 1. Other cells show a similar trend, with a huge increase in ratio observed during secondary necrosis after 350 min.

It is not well understood whether NOX2-generated phagosomal ROS translates into an increase in cytoplasmic or mitochondrial ROS. Studies have measured an increase in cytoplasmic ROS upon silica treatment and attributed this to NOX2 activation. The interpretation of this measurement is difficult because cells were preactivated by either phorbol myristate acetate or lipopolysaccharide before exposure to silica, which results in generalized and nonphagosomal NOX activation and an increase in cellular ROS even before exposure to silica (Kahlenberg *et al.*, 2005; Li *et al.*, 2009; Bauernfeind *et al.*, 2011; Brass *et al.*, 2012). Our experiments were therefore performed without preactivating macrophages. Using ROS sensors, we measured an initial small increase in cytoplasmic ROS upon silica exposure and another larger increase during blebbing associated with apoptosis. No cytoplasmic ROS increase was detected in macrophages exposed to latex particles. Because both latex and silica particles activate NOX2 and phagosomal ROS production in macrophages, it was surprising to see an increase in cytoplasmic ROS only with silica particles. It is possible that ROS generated by silica is capable of passing through the phagosomal membrane to be detected in the cytoplasm. However, because the timing of the appearance of cytoplasmic ROS and the timing of dextran leakage are similar, it seems most likely that phagosomal ROS is leaking into the cytoplasm through a membrane "pore" in the same way as other molecules. The large increase in mitochondrial ROS production during apoptosis appears to be the source of the later increase in cytoplasmic ROS.

In summary, our study provides a comprehensive analysis of spatiotemporal generation of ROS upon exposure of cells to silica and latex particles. We show two distinct events: early, silica-dependent phagosomal ROS generation and later, mitochondria-dependent ROS generation during apoptosis. The early ROS is hypothesized to be the cause of phagosomal membrane damage and leakage leading to the activation of apoptosis. We previously showed a temporal gap of many hours between phagolysosomal leakage and apoptosis (Joshi and Knecht, 2013b). More work is therefore required to understand the linkage between phagolysosomal leakage and the delay in activation of the intrinsic apoptotic pathway.

MATERIALS AND METHODS

Reagents

All chemicals were purchased from Sigma-Aldrich (St. Louis, MO) unless stated otherwise.

Cell culture

MH-S alveolar macrophages (CRL-2019; American Type Culture Collection [ATCC], Manassas, VA) were maintained at 37°C in in RPMI-1640 medium supplemented with 10% heat-inactivated fetal bovine serum (FBS), 10 mM 4-(2-hydroxyethyl)-1-piperazineethanesulfonic acid, 2 mM L-glutamine, and 100 µg/ml ampicillin/streptomycin (complete medium) at 37°C in a 5% CO_2 incubator. Cos7 African green monkey kidney fibroblasts (CRL-1651; ATCC) were maintained in DMEM supplemented with 10% heat-inactivated FBS, 2 mM L-glutamine, 19.4 mM D-glucose, and 100 µg/ml ampicillin/streptomycin at 37°C in a 5% CO_2 incubator. For live-cell imaging experiments, cells were plated at 3×10^4 cells/well in a Lab-Tek II eight-well chamber slide (Thermo Scientific, Waltham, MA) in complete medium 18 h before the start of an experiment.

Particle preparation

Particles were either 3-µm amorphous silica (Alltech/Grace-Davison, Columbia, MO) or 3-µm polystyrene latex (Polysciences, Warrington, PA). Silica particles were baked at 83°C for 18 h to remove any endotoxins. To prepare protein-coated (nonopsonized) particles, 2 mg of silica particles or 100 µl of latex particles was added to 1 ml of 10 mg/ml BSA in particle coating buffer (PCB; 0.15 mM NaCl, 1.8 mM Na_2CO_3, 3.2 mM $NaHCO_3$, pH 9.5) and rotated for 90 min at 37°C. Particles were spun down at 5000 rpm for 2 min, washed three times, and resuspended in 1 ml of phosphate-buffered saline (PBS). A 500-µl amount of these nonopsonized particles was aliquoted and stored at 4°C. To opsonize particles, 5 µl of rabbit anti-BSA antibody (ICL Labs) was added to the remaining 500 µl of nonopsonized particles for 90 min at 37°C. Particles were spun down at 5000 rpm for 2 min and washed three times with PBS. Opsonized particles were resuspended in 500 µl of PBS and stored at 4°C. To determine that particles were coated with antibody, a 1/150 dilution of goat anti-rabbit Texas red secondary antibody was added to 10 µl of opsonized particles and incubated for 30 min at room temperature. The particles were pelleted, resuspended in 100 µl of distilled water, and examined by fluorescence microscopy.

Preparation of FITC-labeled silica particles

Silica particles were opsonized as described in *Particle preparation*. A 500-µl aliquot of opsonized particles was pelleted and resuspended in 400 µl of 0.1 M $NaHCO_3$, pH 8.5. Fifty microliters of 50 mg/ml FITC (dissolved in distilled H_2O) was added to the particles, and the tube was rotated at room temperature for 2 h protected from room light. Particles were pelleted at 5000 rpm for 2 min and resuspended in 500 µl of 0.1 M glycine. The particles were then pelleted and washed once in 500 µl of 0.1 M glycine and once in 500 µl PBS and then stored at 4°C.

Phagolysosomal leakage assay

Cells were plated as described earlier and incubated with 1 mg/ml 4-kDa FITC-dextran or 4-kDa TRITC-dextran in complete medium for 2.5 h at 37°C. For dual-dextran experiments, cells were incubated with 0.5 mg/ml each of 4-kDa FITC-dextran and 4-kDa TRITC-dextran. Cells were then washed twice with complete medium, and then the medium was replaced with CO_2-independent medium (Life Technologies) for imaging. Leakage was measured by drawing a region of interest (ROI) over the nuclear area and measuring mean pixel intensity for every time point (Joshi and Knecht, 2013a)

Detection of ROS

To detect ROS in a phagosome upon particle phagocytosis, silica and latex particles were labeled with H_2HFF-BSA (Life Technologies, Grand Island, NY). Particle coating buffer was deoxygenated by bubbling nitrogen gas for 30 min. A 1-ml amount of deoxygenated PCB was added to a vial containing 1 mg of H_2HFF-BSA. Silica particles (2 mg/ml) or latex particles (100 µl) were added and then incubated for 90 min at 37°C while the tube was being rotated. Meanwhile, PBS was deoxygenated by bubbling nitrogen gas for 30 min. The particles were spun down at 5000 rpm for 2 min, washed three times, and resuspended in 1 ml of deoxygenated PBS. These steps were performed quickly to minimize equilibration of deoxygenated PBS with atmospheric oxygen. A 500-µl amount of these nonopsonized particles was aliquoted and stored at 4°C. To opsonize particles, 5 µl of rabbit anti-BSA antibody (ICL Labs, Portland, OR) was added to the remaining 500 µl of nonopsonized particles and allowed to rotate for 90 min at 37°C. Particles were spun down at 5000 rpm for 2 min and washed three times with deoxygenated PBS. Opsonized particles were resuspended in 500 µl of deoxygenated PBS and stored at 4°C. Labeling efficiency was tested in a similar manner as described earlier. Owing to the sensitivity of H_2HFF to autoxidation, its ability to oxidize upon H_2O_2 addition was tested for each batch of particles. A 10-µg amount of labeled particles was suspended in 500 µl of PBS

and imaged using 488-nm excitation/510-nm emission on a Nikon Ti Eclipse epifluorescence microscope. H_2O_2 at 0.5 M was added to fully oxidize the H_2HFF to check for the oxidative capacity of H_2HFF and set imaging parameters. Note that we do not have calibration standards for H_2HFF fluorescence. Therefore, in an environment containing potentially multiple types of ROS, we do not have a way to determine the amount of any particular ROS. Instead we view this probe as measuring whether there is detectable phagosomal ROS. H_2HFF-labeled particles were used within 48 h of preparation due to autoxidation during storage. Cytoplasmic ROS was detected by loading cells with 10 µM CM-H_2DCFDA (Life Technologies) in complete medium for 30 min at 37°C, after which cells were washed twice and incubated in CO_2-independent medium.

Cell transfection

We plated 1.2×10^5 MH-S murine alveolar macrophages or Cos7 cells in 35-mm Willco glass- bottom dishes (Willco Wells BV, Amsterdam, Netherlands) in 1 ml of complete medium. Twenty-four hours later, the medium was changed to 875 µl of fresh complete medium. Two micrograms of DNA (roGFP2-Orp1 or mito-roGFP2-Orp1; Morgan *et al.*, 2011) was mixed with 100 µl of RPMI incomplete medium for MH-S cells or 100 µl DMEM for Cos7 cells, and 6 µl of FuGeneHD transfection reagent (Promega, Madison, WI) was added. DNA complexes were incubated for 15 min at room temperature and then added to cells. Transient expression of the cells was checked after 10 h and the medium replaced with fresh complete medium. These cells were either used for the experiment or split into eight-well chambered slides for experiments the next day.

Pharmacological inhibitors

Cells were plated in an eight-well chamber slide and loaded with 4-kDa FITC-dextran as described. The chamber was brought to the microscope stage, and DPI was added to bring the final concentration to 0, 5, or 10 µM. Cells were incubated for 30 min and then exposed to 20 µg/cm^2 silica particles and imaged every minute. The average time after particle addition when phagolysosomal leakage was first detected was compared for the different treatments. Similarly, vATPase was inhibited with 150 nM bafilomycin A1 (LC laboratories, Woburn, MA) for 30 min before silica particle addition.

Microscopy

Live-cell microscopy was performed on a Nikon A1R confocal or Nikon Ti Eclipse epifluorescence microscope. Both were fitted with OKO temperature control microscope enclosures (OKO Labs, Pozzuoli, Italy) and stage-top dish incubators for temperature and humidity control (Pathology Devices, Westminster, MD). Both microscopes had motorized stages allowing imaging of multiple fields of view in a well and multiple wells over time. FITC and TRITC images were acquired using a 60×/1.4 numerical aperture Plan APO objective. Dual-excitation and single-emission ratiometric imaging of roGFP2 was done by exciting cells at 405 and 488 nm while collecting emission using a 525/50-nm bandpass filter. For epifluorescence imaging of H_2HFF and TRITC, separate images were collected using GFP and Texas red filter sets using an Andor iXon electron-multiplying charge-coupled device camera (Andor Technology, South Windsor, CT). The hardware for confocal imaging was controlled using Nikon Elements, and epifluorescence was controlled using Micromanager (Edelstein *et al.*, 2010).

Image quantification

Data sets were opened in Fiji for quantification (Schneider *et al.*, 2012). For phagolysosomal dextran fluorescence measurements, an ROI was drawn around a particle, and the mean pixel intensity (MPI) was measured for the TRITC and FITC channels. For nuclear fluorescence, an ROI was drawn on the nuclear region, and the mean pixel intensity of FITC was measured. ROS generation in a phagolysosome with H_2HFF-labeled silica or latex particles was quantified in a similar manner. CM-H_2DCFDA fluorescence was measured by drawing an ROI over the entire cell and measuring MPI over time. Ratiometric image analysis was accomplished using an ROI over an individual cell to measure MPI of the 510-nm emission with 405- and 488-nm excitation. Calculations were done using Excel (Microsoft, Redmond, WA) and data exported to Prism (GraphPad, La Jolla, CA) for statistical analysis and graphing. Pseudocolored ratiometric data sets were generated by dividing images using the image calculator plug-in in Fiji and assigning the Spectrum look-up table.

ACKNOWLEDGMENTS

We thank Tobias Dick at the German Cancer Research Center, Heidelberg, Germany, for the generous gift of roGFP2 sensors and Sergio Grinstein at SickKids, Toronto, Canada, for PX-GFP. We also thank Carol Norris at the University of Connecticut Microscopy Facility for assistance and technical discussion.

REFERENCES

Aderem A, Underhill DM (1999). Mechanisms of phagocytosis in macrophages. Annu Rev Immunol 17, 593–623.

Bauernfeind F, Bartok E, Rieger A, Franchi L, Nuñez G, Hornung V (2011). Cutting edge: reactive oxygen species inhibitors block priming, but not activation, of the NLRP3 inflammasome. J Immunol 187, 613–617.

Becher R, Bucht A, Øvrevik J, Hongslo JK, Dahlman HJ, Samuelsen JT, Schwarze PE (2007). Involvement of NADPH oxidase and iNOS in rodent pulmonary cytokine responses to urban air and mineral particles. Inhal Toxicol 19, 645–655.

Bedard K, Krause K-H (2007). The NOX family of ROS-generating NADPH oxidases: physiology and pathophysiology. Physiol Rev 87, 245–313.

Bohdanowicz M, Cosío G, Backer JM, Grinstein S (2010). Class I and class III phosphoinositide 3-kinases are required for actin polymerization that propels phagosomes. J Cell Biol 191, 999–1012.

Bohdanowicz M, Grinstein S (2010). Vesicular traffic: a Rab SANDwich. Curr Biol 20, R311–R314.

Borges VM, Lopes MF, Falcão H, Leite-Júnior JH, Rocco PRM, Davidson WF, Linden R, Zin WA, DosReis GA (2002). Apoptosis underlies immunopathogenic mechanisms in acute silicosis. Am J Respir Cell Mol Biol 27, 78–84.

Brass DM, Spencer JC, Li Z, Potts-Kant E, Reilly SM, Dunkel MK, Latoche JD, Auten RL, Hollingsworth JW, Fattman CL (2012). Innate immune activation by inhaled lipopolysaccharide, independent of oxidative stress, exacerbates silica-induced pulmonary fibrosis in mice. PLoS One 7, e40789.

Castranova V, Vallyathan V, Ramsey DM, McLaurin JL, Pack D, Leonard S, Barger MW, Ma JY, Dalal NS, Teass A (1997). Augmentation of pulmonary reactions to quartz inhalation by trace amounts of iron-containing particles. Environ Health Perspect 105(Suppl 5), 1319–1324.

Costantini LM, Gilberti RM, Knecht DA (2011). The phagocytosis and toxicity of amorphous silica. PLoS One 6, e14647.

Davis MJ, Gregorka B, Gestwicki JE, Swanson JA (2012). Inducible renitence limits Listeria monocytogenes escape from vacuoles in macrophages. J Immunol 189, 4488–4495.

Davis MJ, Swanson JA (2010). Technical advance: caspase-1 activation and IL-1{beta} release correlate with the degree of lysosome damage, as illustrated by a novel imaging method to quantify phagolysosome damage. J Leukoc Biol 88, 813–822.

DeLeo FR, Allen LA, Apicella M, Nauseef WM (1999). NADPH oxidase activation and assembly during phagocytosis. J Immunol 163, 6732–6740.

Dixon SJ, Stockwell BR (2013). The role of iron and reactive oxygen species in cell death. Nat Chem Biol 10, 9–17.

Dostert C, Petrilli V, Van Bruggen R, Steele C, Mossman BT, Tschopp J (2008). Innate immune activation through Nalp3 inflammasome sensing of asbestos and silica. Science 320, 674–677.

Edelstein A, Amodaj N, Hoover K, Vale R, Stuurman N (2010). Computer control of microscopes using µManager. Curr Protoc Mol Biol, Chapter 14:Unit14 20.

Ellson C, Davidson K, Anderson K, Stephens LR, Hawkins PT (2006). PtdIns3P binding to the PX domain of p40phox is a physiological signal in NADPH oxidase activation. EMBO J 25, 4468–4478.
Esswein EJ, Breitenstein M, Snawder J, Kiefer M, Sieber WK (2013). Occupational exposures to respirable crystalline silica during hydraulic fracturing. J Occup Environ Hyg 10, 347–356.
Fazzi F *et al.* (2014). TNFR1/Phox interaction and TNFR1 mitochondrial translocation thwart silica-induced pulmonary fibrosis. J Immunol 192, 3837–3846.
Fisher AB (2009). Redox signaling across cell membranes. Antioxid Redox Signal 11, 1349–1356.
Ghio AJ, Kennedy TP, Whorton AR, Crumbliss AL, Hatch GE, Hoidal JR (1992). Role of surface complexed iron in oxidant generation and lung inflammation induced by silicates. Am J Physiol 263, L511–L518.
Gilberti RM, Joshi GN, Knecht DA (2008). The phagocytosis of crystalline silica particles by macrophages. Am J Respir Cell Mol Biol 39, 619–627.
Gilberti RM, Knecht DA (2015). Macrophages phagocytose nonopsonized silica particles using a unique microtubule-dependent pathway. Mol Biol Cell 26, 518–529.
Guo J, Gu N, Chen J, Shi T, Zhou Y, Rong Y, Zhou T, Yang W, Cui X, Chen W (2013). Neutralization of interleukin-1 beta attenuates silica-induced lung inflammation and fibrosis in C57BL/6 mice. Arch Toxicol 87, 1963–1973.
Hampton M, Kettle A, Winterbourn C (1998). Inside the neutrophil phagosome: oxidants, myeloperoxidase, and bacterial killing. Blood 92, 3007.
Henry RM, Hoppe AD, Joshi N, Swanson JA (2004). The uniformity of phagosome maturation in macrophages. J Cell Biol 164, 185–194.
Hornung V, Bauernfeind F, Halle A, Samstad EO, Kono H, Rock KL, Fitzgerald KA, Latz E (2008). Silica crystals and aluminum salts activate the NALP3 inflammasome through phagosomal destabilization. Nat Immunol 9, 847–856.
Humphries WH, Szymanski CJ, Payne CK (2011). Endo-lysosomal vesicles positive for Rab7 and LAMP1 are terminal vesicles for the transport of dextran. PLoS One 6, e26626.
Joshi GN, Knecht DA (2013a). Multi-parametric analysis of cell death pathways using live-cell microscopy. Curr Protoc Toxicol 58, Unit 4.40.
Joshi GN, Knecht DA (2013b). Silica phagocytosis causes apoptosis and necrosis by different temporal and molecular pathways in alveolar macrophages. Apoptosis 18, 271–285.
Kahlenberg JM, Lundberg KC, Kertesy SB, Qu Y, Dubyak GR (2005). Potentiation of caspase-1 activation by the P2 7 receptor is dependent on TLR signals and requires NF-B-driven protein synthesis. J Immunol 175, 7611–7622.
Kalyanaraman B (2013). Teaching the basics of redox biology to medical and graduate students: oxidants, antioxidants and disease mechanisms. Redox Biol 1, 244–257.
Kalyanaraman B, Darley-Usmar V, Davies KJA, Dennery PA, Forman HJ, Grisham MB, Mann GE, Moore K, Roberts LJ, Ischiropoulos H (2012). Measuring reactive oxygen and nitrogen species with fluorescent probes: challenges and limitations. Free Radic Biol Med 52, 1–6.
Kang JL, Go YH, Hur KC, Castranova V (2000). Silica-induced nuclear factor-kappaB activation: involvement of reactive oxygen species and protein tyrosine kinase activation. J Toxicol Environ Health A 60, 27–46.
Kon K, Kim J-S, Uchiyama A, Jaeschke H, Lemasters JJ (2010). Lysosomal iron mobilization and induction of the mitochondrial permeability transition in acetaminophen-induced toxicity to mouse hepatocytes. Toxicol Sci 117, 101–108.
Kurz T, Eaton JW, Brunk UT (2011). The role of lysosomes in iron metabolism and recycling. Int J Biochem Cell Biol 43, 1686–1697.
Li XJ, Tian W, Stull ND, Grinstein S, Atkinson S, Dinauer MC (2009). A fluorescently tagged C-terminal fragment of p47phox detects NADPH oxidase dynamics during phagocytosis. Mol Biol Cell 20, 1520–1532.
Lukacs GL, Rotstein OD, Grinstein S (1990). Phagosomal acidification is mediated by a vacuolar-type H(+)-ATPase in murine macrophages. J Biol Chem 265, 21099–21107.
Maejima I *et al.* (2013). Autophagy sequesters damaged lysosomes to control lysosomal biogenesis and kidney injury. EMBO J 32, 2336–2347.
Morgan B, Sobotta MC, Dick TP (2011). Measuring E(GSH) and H(2)O(2) with roGFP2-based redox probes. Free Radic Biol Med 51, 1943–1951.
Musset B, Cherny VV, Morgan D, DeCoursey TE (2009). The intimate and mysterious relationship between proton channels and NADPH oxidase. FEBS Lett 583, 7–12.
Oberdörster G, Oberdörster E, Oberdörster J (2005). Nanotoxicology: an emerging discipline evolving from studies of ultrafine particles. Environ Health Perspect 113, 823–839.
Persson HL (2005). Iron-dependent lysosomal destabilization initiates silica-induced apoptosis in murine macrophages. Toxicol Lett 159, 124–133.
Price MO, McPhail LC, Lambeth JD, Han C-H, Knaus UG, Dinauer MC (2002). Creation of a genetic system for analysis of the phagocyte respiratory burst: high-level reconstitution of the NADPH oxidase in a nonhematopoietic system. Blood 99, 2653–2661.
Rojanasakul Y, Ye J, Chen F, Wang L, Cheng N, Castranova V, Vallyathan V, Shi X (1999). Dependence of NF-kappaB activation and free radical generation on silica-induced TNF-alpha production in macrophages. Mol Cell Biochem 200, 119–125.
Ross MH, Murray J (2004). Occupational respiratory disease in mining. Occup Med (Lond) 54, 304–310.
Russell DG, VanderVen BC, Glennie S, Mwandumba H, Heyderman RS (2009). The macrophage marches on its phagosome: dynamic assays of phagosome function. Nat Rev Immunol 9, 594–600.
Sandberg WJ, Låg M, Holme JA, Friede B, Gualtieri M, Kruszewski M, Schwarze PE, Skuland T, Refsnes M (2012). Comparison of non-crystalline silica nanoparticles in IL-1β release from macrophages. Part Fibre Toxicol 9, 32.
Sato T, Shimosato T, Alvord WG, Klinman DM (2008). Suppressive oligodeoxynucleotides inhibit silica-induced pulmonary inflammation. J Immunol 180, 7648–7654.
Savina A, Jancic C, Hugues S, Guermonprez P, Vargas P, Moura IC, Lennon-Duménil A-M, Seabra MC, Raposo G, Amigorena S (2006). NOX2 controls phagosomal pH to regulate antigen processing during crosspresentation by dendritic cells. Cell 126, 205–218.
Schneider CA, Rasband WS, Eliceiri KW (2012). NIH Image to ImageJ: 25 years of image analysis. Nat Methods 9, 671–675.
Scott CC (2005). Phosphatidylinositol-4,5-bisphosphate hydrolysis directs actin remodeling during phagocytosis. J Cell Biol 169, 139–149.
Shen HM, Zhang Z, Zhang QF, Ong CN (2001). Reactive oxygen species and caspase activation mediate silica-induced apoptosis in alveolar macrophages. Am J Physiol Lung Cell Mol Physiol 280, L10–L17.
Srivastava KD, Rom WN, Jagirdar J, Yie T-A, Gordon T, Tchou-WOng K-M (2002). Crucial role of interleukin-1beta and nitric oxide synthase in silica-induced inflammation and apoptosis in mice. Am J Respir Crit Care Med 165, 527–533.
Suh C-I, Stull ND, Li XJ, Tian W, Price MO, Grinstein S, Yaffe MB, Atkinson S, Dinauer MC (2006). The phosphoinositide-binding protein p40phox activates the NADPH oxidase during FcgammaIIA receptor-induced phagocytosis. J Exp Med 203, 1915–1925.
Swanson JA, Hoppe AD (2004). The coordination of signaling during Fc receptor-mediated phagocytosis. J Leukoc Biol 76, 1093–1103.
Thibodeau MS, Giardina C, Knecht DA, Helble J, Hubbard AK (2004). Silica-induced apoptosis in mouse alveolar macrophages is initiated by lysosomal enzyme activity. Toxicol Sci 80, 34–48.
Tian W, Li XJ, Stull ND, Ming W, Suh CI, Bissonnette SA, Yaffe MB, Grinstein S, Atkinson SJ, Dinauer MC (2008). Fc R-stimulated activation of the NADPH oxidase: phosphoinositide-binding protein p40phox regulates NADPH oxidase activity after enzyme assembly on the phagosome. Blood 112, 3867–3877.
Vallyathan V, Shi XL, Dalal NS, Irr W, Castranova V (1988). Generation of free radicals from freshly fractured silica dust. Potential role in acute silica-induced lung injury. Am Rev Respir Dis 138, 1213–1219.
VanderVen BC, Yates RM, Russell DG (2009). Intraphagosomal measurement of the magnitude and duration of the oxidative burst. Traffic 10, 372–378.
Wang L, Antonini JM, Rojanasakul Y, Castranova V, Scabilloni JF, Mercer RR (2003). Potential role of apoptotic macrophages in pulmonary inflammation and fibrosis. J Cell Physiol 194, 215–224.
Winterbourn CC, Hampton MB, Livesey JH, Kettle AJ (2006). Modeling the reactions of superoxide and myeloperoxidase in the neutrophil phagosome: implications for microbial killing. J Biol Chem 281, 39860–39869.
Winterbourn CC, Kettle AJ (2013). Redox reactions and microbial killing in the neutrophil phagosome. Antioxid Redox Signal 18, 642–660.
Wong-Ekkabut J, Xu Z, Triampo W, Tang I-M, Tieleman DP, Monticelli L (2007). Effect of lipid peroxidation on the properties of lipid bilayers: a molecular dynamics study. Biophys J 93, 4225–4236.
Zeidler PC, Roberts JR, Castranova V, Chen F, Butterworth L, Andrew ME, Robinson VA, Porter DW (2003). Response of alveolar macrophages from inducible nitric oxide synthase knockout or wild-type mice to an in vitro lipopolysaccharide or silica exposure. J Toxicol Environ Health A 66, 995–1013.